Title

Seasonal and synoptic oceanographic changes influence the larval biodiversity of a retentive upwelling shadow

Authors

Satterthwaite, Erin V
Morgan, Steven G
Ryan, John P
et al.

Publication Date

2020-03-01

DOI

10.1016/j.pocean.2019.102261

Peer reviewed

Progress in Oceanography 182 (2020) 102261

Contents lists available at ScienceDirect

Progress in Oceanography

journal homepage: www.elsevier.com/locate/pocean

Seasonal and synoptic oceanographic changes influence the larval biodiversity of a retentive upwelling shadow

Erin V. Satterthwaite[a,b,*], Steven G. Morgan[a,b], John P. Ryan[c], Julio B.J. Harvey[c], Robert C. Vrijenhoek[c]

[a] Bodega Marine Laboratory, University of California Davis, Bodega Bay, CA 94923, USA
[b] Department of Environmental Science and Policy, University of California Davis, Davis, CA 95616, USA
[c] Monterey Bay Aquarium Research Institute, Moss Landing, CA 95039, USA

ARTICLE INFO

Keywords:
Larval assemblage
Meroplankton
Zooplankton
Upwelling shadow
Currents
Seasonality
Monterey Bay
Biodiversity
Biological oceanography

ABSTRACT

Understanding sources of variability in larval supply and transport is integral to the dynamics, structure and effective management of marine populations and communities. Yet, a barrier to this understanding is the high variability in the supply and transport of marine larvae, especially in upwelling regions where wind forcing causes dynamic circulation. Since larvae of many species complete development close to shore, resolving the relationship between oceanographic processes and nearshore larval assemblages is essential to better understand larval transport in highly productive upwelling regions. The goal of our study was to examine the effects of variation in upwelling and relaxation dynamics on the nearshore larval assemblage in northern Monterey Bay. To determine how seasonal and daily upwelling and relaxation dynamics influence the nearshore larval assemblage, we surveyed distributions of marine larvae and physical, environmental factors along a cross-shelf transect in northern Monterey Bay, USA, during August and October of 2013.

Conditions in August and October differed in temperature, salinity, stratification, and chlorophyll-*a* fluorescence. Richness and diversity of the larval assemblage did not change appreciably, but the abundance and composition of species shifted after the influx of offshore waters. Specifically, nearshore taxa were more abundant during August, which was characterized by strong upwelling conditions, and especially more abundant with increased wind forcing leading to a retentive upwelling shadow in the northern bay. Conversely, offshore taxa were more abundant during October, which was characterized by weakened upwelling and the persistent influx of offshore water. Our study suggests that relationships between larval taxa, life history characteristics, and water types provide insights into water mass history, circulation and larval recruitment in highly dynamic upwelling regions.

1. Introduction

Larval dispersal is crucial to the ecology and evolution of marine animals because it affects their persistence, population dynamics, and community structure. Understanding how environmental factors affect the distributions and abundance of larvae and the spatial and temporal scales involved is integral to effective ecosystem-based management and marine spatial planning (Levin, 2006). Yet, the highly variable supply of marine larvae, directly influenced by physical processes operating at varying spatial and temporal scales, is notoriously difficult to characterize (Underwood and Fairweather, 1989).

One such physical process is wind forcing, which has been shown to dramatically alter circulation patterns and influence larval transport. In eastern boundary upwelling systems, including the California Current System, equatorward winds combined with the earth's rotation (Coriolis) drive surface waters offshore, and draw deep, cold, nutrient-rich water to the surface (Huyer, 1983). When prevailing winds weaken (i.e., relaxation), surface water may flow poleward and onshore, resulting in downwelling at the coast (Hickey, 1998). Since larvae of many species in upwelling regions complete development close to shore (< 6 km, Morgan et al., 2009; Shanks and Shearman, 2009; Bartilotti et al., 2014; Fisher et al., 2014; Morgan, 2014), resolving nearshore oceanographic processes (e.g., eddies, fronts, retention zones) and circulation is essential to resolve larval transport mechanisms (Pineda et al., 2007). Heterogeneity in nearshore circulation patterns arises from the interaction between wind forcing (i.e., upwelling and

* Corresponding author at: Bodega Marine Laboratory, University of California Davis, Bodega Bay, CA 94923, USA.
E-mail address: evsatterthwaite@ucdavis.edu (E.V. Satterthwaite).

https://doi.org/10.1016/j.pocean.2019.102261
Received 29 January 2019; Received in revised form 23 August 2019; Accepted 30 December 2019
Available online 10 January 2020

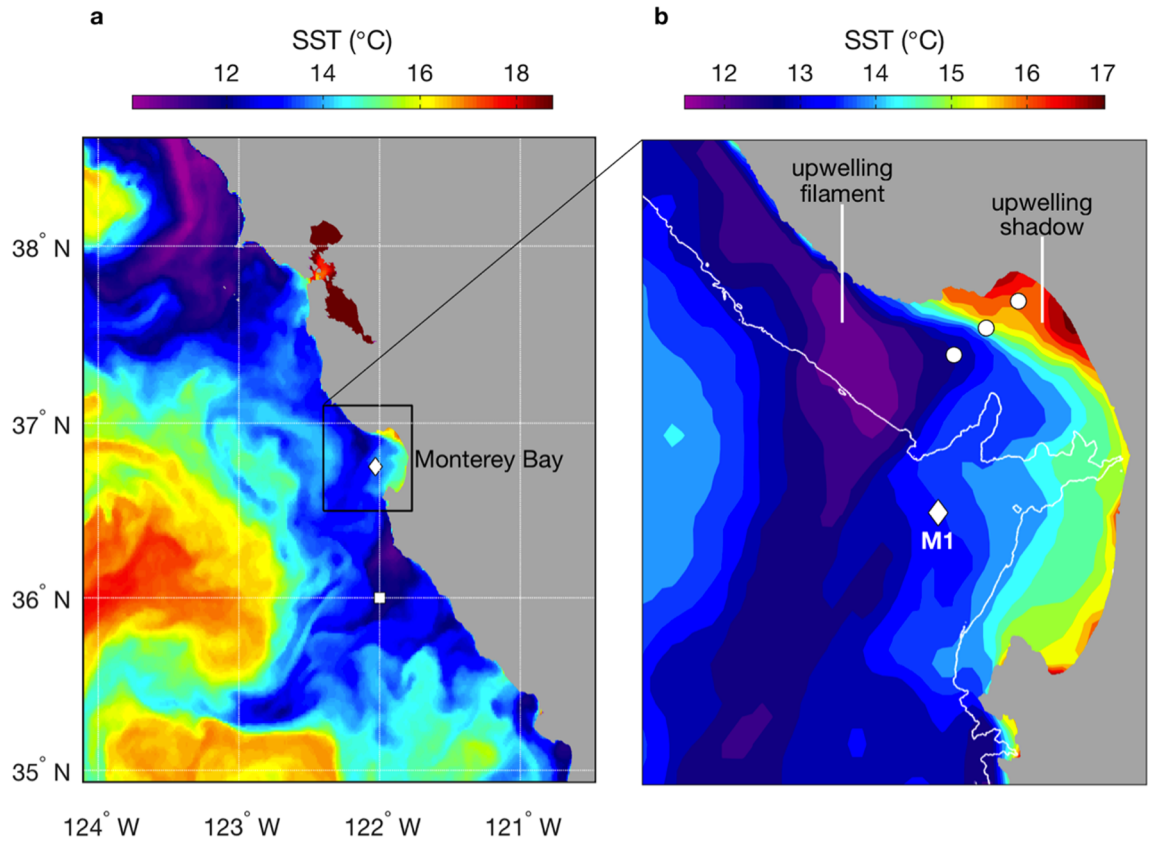

Fig. 1. Sea Surface Temperature (SST) in Monterey Bay and vicinity on 2 October 2013 21:37 UTC. (a) SST along the central Californian coast. The location nearest Monterey Bay for which the NOAA upwelling index is computed (36°N, 122°W; white square; data in Fig. 2a) and the locations of the MBARI M1 buoy (white diamond; data in Fig. 2b–e) are indicated. The M1 mooring is located in the channel of Monterey Submarine Canyon at 1000 m depth. (b) SST in Monterey Bay. White circles mark the locations of CTD casts and water sampling stations that were repeatedly sampled for meroplankton during August and October 2013. AUV surveys were conducted parallel to this transect. A white contour represents the 100 m isobath. SST data in the right panel (b) are a subset of the data in the left panel (a).

relaxation dynamics), coastal geometry (e.g. bays, headlands), and bathymetry (Huyer, 1983; Hickey, 1998; Gan and Allen, 2002).

Monterey Bay, California is an ideal location to study heterogeneity in nearshore circulation and the effects on larval assemblages because it is situated in the dynamic upwelling environment of the central California Current System. It is the largest open bay along the west coast of the USA and is bisected by Monterey Canyon (Fig. 1). Monterey Bay receives highly variable inputs of relatively saline, recently upwelled water during periods of northwesterly wind forcing, and less saline offshore water during periods of upwelling relaxation, when northwesterly winds weaken or reverse (Graham and Largier, 1997). When there is strong northwesterly wind forcing, plumes of upwelled water originating in the upwelling center off Point Año Nuevo flow southward across the mouth of Monterey Bay, or bifurcate curving into the bay leading to retention in the northern bay, known as an “upwelling shadow” (Rosenfeld et al., 1994; Graham and Largier, 1997; Ryan et al., 2014b). Enhanced residence time in the upwelling shadow leads to greater thermal heating and stratification (Graham and Largier, 1997). As upwelling winds become weaker and more variable, typical of fall, the influx of offshore, low salinity waters increases in frequency. Consequently, the nearshore oceanic environment of Monterey Bay changes significantly with highly variable influxes of these primary source waters. Thus, there is high temporal variation in the frequency and duration of upwelling and relaxation events affecting the circulation of Monterey Bay, which occurs at three specific scales: synoptic wind forcing (days to weeks), alongshore variation in forcing mechanisms by mesoscale circulation patterns (weeks to months), and the annual signal from the fluctuation in the wind strength (years) (Largier et al., 1993).

In the California Current, there are considerable effects of source water variability on phytoplankton, zooplankton, and larval communities. For example, during upwelling, when nearshore currents interact with headlands or coastal promontories, leeward eddies form, increasing water mass residence times, and enhancing surface warming. The resulting surface warming and enhanced stratification can lead to phytoplankton blooms within the upwelling shadow (e.g., Ryan et al., 2008, 2017). In addition, larvae of many taxa become entrained and accumulate in headland-generated oceanographic features of Bodega Bay (Roughan et al., 2005; Morgan et al., 2011), Gulf of the Farallones (Wing et al., 1998), and Monterey Bay (Graham et al., 1992; Harvey et al., 2012; Ryan et al., 2014a). Consequently, larval settlement is greater in the lee of coastal headlands, such as Point Reyes and Bodega Head, than along the exposed surrounding coastline (Wing et al., 2003; Mace and Morgan, 2006). In addition, variable transport of offshore water masses into bays is another major factor that affects the oceanographic conditions of nearshore areas along the California coast (Graham and Largier, 1997). During upwelling favorable (northwesterly) wind forcing, cool and salty upwelled water enters bays, whereas during relaxation or reversal of upwelling winds, fresher offshore water is transported shoreward into bays (Rosenfeld et al., 1994; Graham and Largier, 1997; Ramp et al., 2005). The influx of fresher, offshore water significantly affects the phytoplankton assemblage (Bolin and Abbott, 1963; Ryan et al., 2014b). However, the effect on larval assemblages has not been well studied even though upwelling shadows, due to their highly productive and retentive nature, play an important role in the nearshore ecology of recruitment-limited upwelling regions.

Consequently, the goal of our study was to examine the effects of variation in upwelling and relaxation dynamics on the nearshore larval assemblage in northern Monterey Bay. Specifically, we characterized the monthly (seasonal) and daily (synoptic) variation in upwelling and

relaxation dynamics on the source water composition in the bay as well as the effect of these oceanographic changes on larval assemblages and phytoplankton concentrations in northern Monterey Bay. We focus on the seasonal variation in oceanography in relation to the larval assemblage in order to elucidate the effect of broad scale oceanographic processes on marine larval assemblages, and we use the variation in daily environmental conditions and larval abundances to elucidate finer scale temporal patterns. Characterizing the relationship between oceanographic conditions and the associated larval assemblages contributes to a more holistic understanding of the nearshore biophysical dynamics of upwelling regions.

2. Materials and methods

2.1. Field surveys

We conducted two cruises in northern Monterey Bay (Fig. 1a) during late summer (12 to 16 August 2013) and early fall (22 to 25 October 2013) aboard the R/V Rachel Carson. We repeatedly sampled three stations ranging from 20 m to 60 m deep along an 8-km transect that extended from the inner to the outer bay, and intended to cross upwelled and upwelling shadow waters (Fig. 1b). At each station, we measured temperature, salinity and depth (Sea-Bird Scientific SBE 911Plus CTD), oxygen (Sea-Bird Scientific SBE 43), and chlorophyll-*a* fluorescence (Wetlabs WetStar WS3S Fluorometer) throughout the water column with a profiling CTD package (Sea-Bird Scientific, Bellevue, Washington) to characterize potential links between larval assemblages and hydrographic properties of the water column.

The Monterey Bay Aquarium Research Institute (MBARI) autonomous underwater vehicle (AUV) *Dorado* was deployed concurrently with both expeditions to measure physical, optical, and chemical oceanographic characteristics along the transect during each day of sampling. CTD data from the AUV were used to examine water column properties and stratification across the survey transect. AUV sensor data used in this study were from a Sea-Bird Scientific SBE-25 CTD and a Hobi Labs HydroScat-2 (optical backscatter and chlorophyll fluorescence). Five daily AUV surveys were conducted between 12 and 16 August 2013, and four daily surveys were conducted between 22 and 25 October 2013. All sensors were calibrated before deployment.

We concurrently collected meroplankton above, within, and below the chlorophyll-*a* maximum, with a gas-powered pump. The terminal end of a 6-cm diameter hose from the pump was attached to the outside of the CTD package frame. Chlorophyll-*a* layer and pump sampling depths were determined in real time by monitoring CTD environmental data during each cast. We pumped 240 L of seawater per min for 10 min and sampled 2.4 m^3 of seawater per depth. Samples were filtered through a 115-μm-mesh plankton net that was suspended over the side of the ship's rail, with the cod end submerged beneath the sea surface. Samples were preserved in 95% ethanol.

2.2. Physical data analysis

Seasonal variation in regional wind forcing during 2013 was examined using the NOAA monthly mean upwelling index, which is computed for a series of locations along the margin of the northeastern Pacific Ocean. Index data from the location nearest to Monterey Bay (Fig. 1a) are presented. Upwelling index data were obtained from the NOAA ERDDAP server (https://coastwatch.pfeg.noaa.gov/erddap/index.html). Seasonal and episodic variations in temperature, salinity, water velocity, and wind forcing at the mouth of Monterey Bay were examined using CTD and acoustic Doppler current profiler (ADCP) data from the MBARI M1 mooring (Fig. 1). Descriptions of the instruments and data processing methods for M1 have been published (Ryan et al., 2009). Regional sea surface temperature (SST) coverage during the study periods was examined using NOAA POES SST (https://coastwatch.pfeg.noaa.gov/erddap/index.html). Due to prevalent cloud and fog cover, coverage was inadequate to examine regional variations during the study periods. However, a SST image acquired before the second field program is used to illustrate regional upwelling patterns and the upwelling shadow in relation to the spatial sampling plan (Fig. 1). AUV data processing methods have been published (Ryan et al., 2010). For this study, CTD data were analyzed in two ways to provide context for meroplankton data: (1) a temperature-salinity plot was produced to examine the degree of overlap in water properties during the two study periods, and (2) daily vertical sections of temperature, salinity, and chlorophyll-*a* fluorescence were computed for each study period to examine changes in the spatial structure and stratification of the water column along the transect.

2.3. Biological data analysis

2.3.1. Phytoplankton

Chlorophyll-*a* fluorescence from ship CTD casts was compared between expeditions in August and October. A histogram and Shapiro-Wilk test for normality revealed that fluorescence values were not normally distributed, so data were log transformed to meet the assumptions of normality (Campbell, 1995). A F-test was then conducted on the log-transformed data to ensure homogeneity of variances between months. Then, a *t*-test was run on the log-transformed chlorophyll data to detect differences between August and October sampling periods. Phytoplankton species compositions and relative abundances were obtained from a sample collected in the upper 3m of the water column using a 20-μm mesh net at the Santa Cruz Municipal Wharf during each sampling period (14 August 2013 and 23 October 2013) to provide a weekly snapshot of the phytoplankton community. Relative abundances of phytoplankton species were categorized as follows: rare ($< 1\%$ of sample), present (1–9% of sample), common (10–49% of sample), or abundant ($\geq 50\%$ of sample). The samples were analyzed at the University of California Santa Cruz (Kudela Lab), and data were provided by the Ocean Data Center (http://oceandatacenter.ucsc.edu/PhytoBlog/). Descriptions of the phytoplankton sampling methods have been published (Jester et al., 2009).

2.3.2. Meroplankton assemblage

We split samples with a Folsom plankton splitter and identified the developmental stages of meroplankton using a dissecting microscope. Larvae initially identified to species were subsequently grouped to class or order for data analysis due to low overall abundances. We then grouped larvae into early and late stages. In addition, we used high throughput DNA sequencing of the mitochondrial cytochrome-*c*-oxidase subunit-I (*COI*) gene to resolve taxa that were difficult to identify morphologically to the species level. Taxonomic names were assigned to OTU sequences by comparing them to custom reference sequence databases using the Basic Local Alignment Search Tool (BLAST). Descriptions of the complete molecular methods have been published (Harvey et al., 2018).

To conceptualize differences in meroplankton assemblages between sampling months and days, the meroplankton assemblages were visualized using nonmetric multidimensional scaling (NMDS) and NMDS scores for individual taxa were calculated. To test for significant differences in meroplankton assemblages between months and days we used PERMANOVA analysis (adonis function, 9999 permutations). To determine which specific taxa were most different between sampling periods, similarity percentages were calculated using SIMPER (SIMilarity PERcentage; Clarke and Warwick, 2001). NMDS, PERMANOVA and SIMPER were run in R with the package vegan (Oksanen et al., 2016).

2.3.3. Richness and diversity

Richness and diversity of larval taxa were calculated for each sample. Shannon-Weaver diversity indices were calculated in R (R Core Team, 2017) using the community ecology package vegan (Oksanen

et al., 2016). Histograms and Shapiro-Wilk tests for normality revealed that richness and diversity for both sampling periods were normally distributed. In addition, a F-test was conducted to ensure variances were similar between months. A *t*-test was run to compare richness and diversity between sampling periods.

2.3.4. Composition and total larval abundance

For all taxa and stages collected, we calculated the mean and standard error of each taxon for both sampling periods. Larval distributions are inherently patchy, resulting in zero-inflated data. Zeros in count data may be caused by either true zero counts or false zero counts. True zero counts occur when the species is not present due to an ecological phenomenon, such as poor habitat or demography. False zero counts occur due to chance and may arise when a species does not fill an available niche or when a sampling method is inadequate (Martin et al., 2005). Because of the large number of zero counts and since the variance was much larger than the mean (overdispersion) for most of the larval taxa, zero-inflated negative binomial generalized linear models were used to assess the importance of sampling period and days within each month as a predictor variable for both count (with a log link) and zero data. In these models, the presence or absence (zero) of a count are modeled separately. The pscl (Zeileis et al., 2008) and MASS (Venables and Ripley, 2002) packages in R were used for these analyses.

2.3.5. Daily larval abundance in relation to daily environmental variables

In order to understand how the seasonal patterns were related to the daily variations in the oceanographic conditions and larval assemblages, we assessed the daily environmental conditions and aggregated sample level to daily larval abundances. To explore the environmental factors that could have been driving differences in daily larval abundances, the wind data from M1 buoy and environmental data (depth/distance from seafloor, water temperature, salinity, oxygen, and chlorophyll-*a* fluorescence) from the profiling CTD attached near the meroplankton pump were used for analysis of daily variation in larval abundances.

Wind speed and direction data from 2013 were obtained from the M1 buoy (Buoy 46092) located in the center of Monterey Bay and was accessed from the National Data Buoy Center website (http://www.ndbc.noaa.gov/). Alongshore and cross-shore wind components were calculated from the wind speed and direction obtained from the M1 buoy relative to the mean coastline angle near Monterey Bay (335°), positive directions represent poleward and onshore. Mean, maximum, and minimum wind speed and median wind direction were calculated for each sampling day (24 h prior to the end of each sampling day-12:00 pm day prior to 12:00 pm day of sampling). Similarly, the average, median, maximum, and minimum values were calculated for alongshore and cross-shore speeds for each sampling day. In addition, the mean, maximum, and minimum values were calculated for all environmental variables from the profiling CTD (salinity, water temperature, oxygen, distance from seafloor, and chlorophyll-*a* fluorescence) for each day.

The daily values of environmental variables (wind parameters, salinity, water temperature, oxygen, distance from seafloor, and chlorophyll-*a* fluorescence) were compared to the total daily abundance of each taxon using Spearman rank-order correlation since distributions of larvae were non-normal (R Core Team, 2017).

3. Results

3.1. Temporal variation in oceanographic conditions

3.1.1. Seasonal

The depth of isotherms and isohalines at the mouth of Monterey Bay reflects the seasonal cycle of regional upwelling strength (Fig. 2a). Shoaling isopleths during April – July 2013 indicate the strongest upwelling period of 2013 (Fig. 2a-c). Warming and freshening of the water column during August to October (Fig. 2b-c, Fig. 3), the months described as the fall "oceanic season" (Pennington and Chavez, 2000), are associated with weakening of upwelling and deepening of isopleths (Fig. 2, Fig. 4). The key hydrographic distinctions of the October study period relative to August include a thicker and warmer mixed layer (Fig. 2b) and lower salinity (Fig. 2c) at the mouth of the bay, consistent with weaker upwelling favorable winds (Fig. 4) and greater influence of fresher offshore water entering the bay (Fig. 3, Fig. 5). The salinity changes are oceanographic and not related to freshwater runoff into the bay. Circulation at the mouth of Monterey Bay exhibited a stronger poleward (northward) flow prior to the October study, compared to the August study (Fig. 2d), and a stronger onshore (eastward) flow during the October sample period, compared to the August study (Fig. 2e). Onshore flow speeds of 10–20 cm/s would transport waters about 9–17 km onshore in a day, thereby delivering offshore waters and associated planktonic larvae to inner Monterey Bay where larvae were sampled.

August and October temperature-salinity domains along the sampling transect were distinct (Fig. 3), indicating different hydrography. The water column in the upwelling shadow had higher salinity in August, consistent with the relatively strong influence of upwelled water. Supply of upwelled water and surface warming led to a large temperature range in August which was twice that of October (Fig. 3). The stronger vertical thermal stratification in August is also evident in the M1 time-series (Fig. 2b). During each sampling period, meroplankton were collected throughout the temperature and salinity range sampled, except from deep shelf water (coldest and most saline) and the lowest salinity features that represented a small portion of the AUV transect data (Fig. 3).

Examined in the spatial context of the sampling transect, the change in stratification indicated in the T-S plot (Fig. 3) extended across the entire survey domain, as did the observed decrease in salinity (Fig. 5). Further, the primary spatial orientation of isohalines toward the offshore side of the transect changed from horizontal to vertical between August and October (Fig. 5), consistent with the influx of offshore, low-salinity water before and during October. The influx of offshore water is indicated in the M1 time series, as low salinity events in the upper 60 m during September–October (Fig. 2c). This pattern of low salinity water entering Monterey Bay has been previously observed during circulation responses to relaxation of upwelling (Graham and Largier, 1997; Ryan et al., 2010).

3.1.2. Daily

In addition to seasonal changes, there was marked synoptic variability in upwelling, with fluctuations between upwelling and relaxation conditions occurring over several days. Upwelling-favorable winds increased through the August sampling period, with the strongest alongshore winds (~12 m/s) late on 14 August, followed by weakened winds on 15 August (Fig. 4). The stratification was strong throughout the entire August sampling period in regard to both temperature and salinity, and the chlorophyll-*a* maximum layer consistently occurred at the pycnocline in the middle of the water column (Fig. 5a-e). More saline waters were present deep and offshore in Monterey Bay on 15 to 16 August 2013 (Fig. 5d-e).

Conversely, the October sampling period was characterized by weakened upwelling, with weak alongshore winds (often < 4 m/s) but stronger, more variable cross-shore winds throughout the sampling period (Fig. 4). During all sampling days, there was a strong signature of offshore source water flowing into the sampling domain as evidenced by the low salinity water present offshore (Fig. 5f-i). Yet, the distance along the transect that the offshore source water intruded varied on a daily timescale (Fig. 5f-i). The influx of offshore water was strongest and closest to shore on 22 Oct 2013 (Fig. 5f), receded from shore until

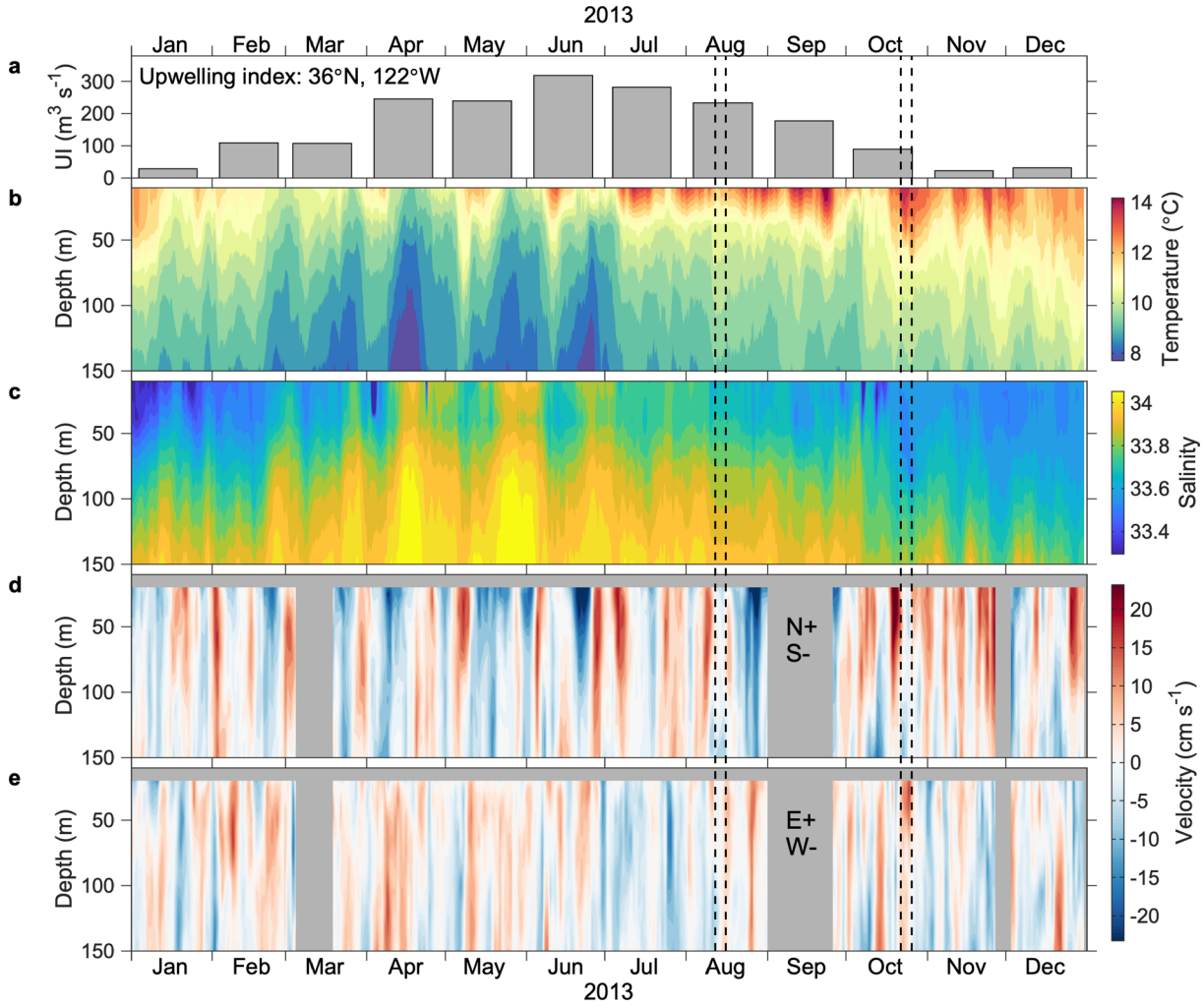

Fig. 2. Monthly oceanographic conditions in northern Monterey Bay during 2013. Dashed vertical lines indicate sampling expedition durations (12–16 August and 22–25 October). (a) Monthly mean upwelling index (36°N, 122°W; white square in Fig. 1a). Temperature (b) and salinity (c) at mooring M1 (white diamonds in Fig. 1). Meridional (d; north–south) and zonal (e; east–west) current velocities at mooring M1; signs corresponding to direction are noted in each.

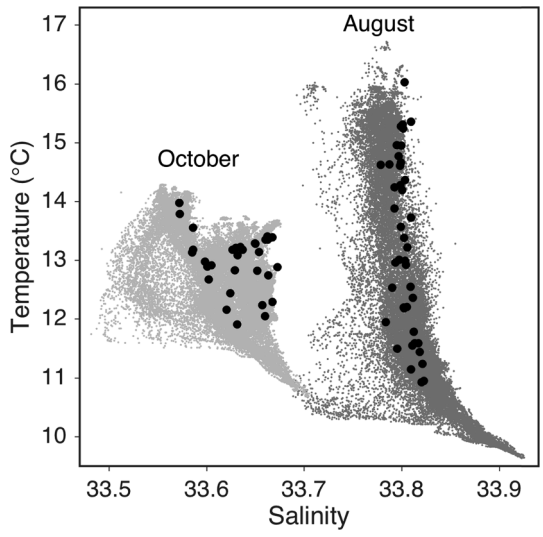

Fig. 3. Temperature-salinity plot of data from CTD casts and AUV *Dorado* data collected along the meroplankton sampling transect in northern Monterey Bay, August and October 2013. Gray point clouds represent AUV data, and solid black circles represent ship CTD values specific to meroplankton water samples.

24 Oct 2013 (Fig. 5g-h), and slightly moved toward shore again on 25 Oct 2013 (Fig. 5i). The influx and slight recession of offshore waters were reflected in the dynamics of the chlorophyll-*a* fluorescence maximum layer. The chlorophyll-*a* maxima occurred at the surface to about 10 m depth for all sampling days in October (Fig. 5f-i). Yet, the cross-shore distance of the maxima moved from nearshore on 22 and 23 October 2013 to offshore on 24 October 2013 and then to the middle of the bay on 25 October 2013.

3.2. Phytoplankton

3.2.1. Seasonal

Higher chlorophyll-*a* fluorescence during the August sampling period was evident in AUV sections of fluorometric chlorophyll-*a* data (Fig. 5), consistent with ship CTD profile data, the mean of which was greater in August than October ($t(1,74) = 4.48$, $p < 0.0001$). Phytoplankton species compositions at Santa Cruz Wharf differed between sampling periods. In August, the diatom *Pseudo-nitzschia* was abundant (representing between 50% and 100% of the sample) and dinoflagellates were rare (< 1%). In October, all diatoms, including *Pseudo-nitzschia*, were rare (< 1%) and dinoflagellates (*Cochlodinium* and *Ceratium*) were common (representing between 20 and 98% of the sample).

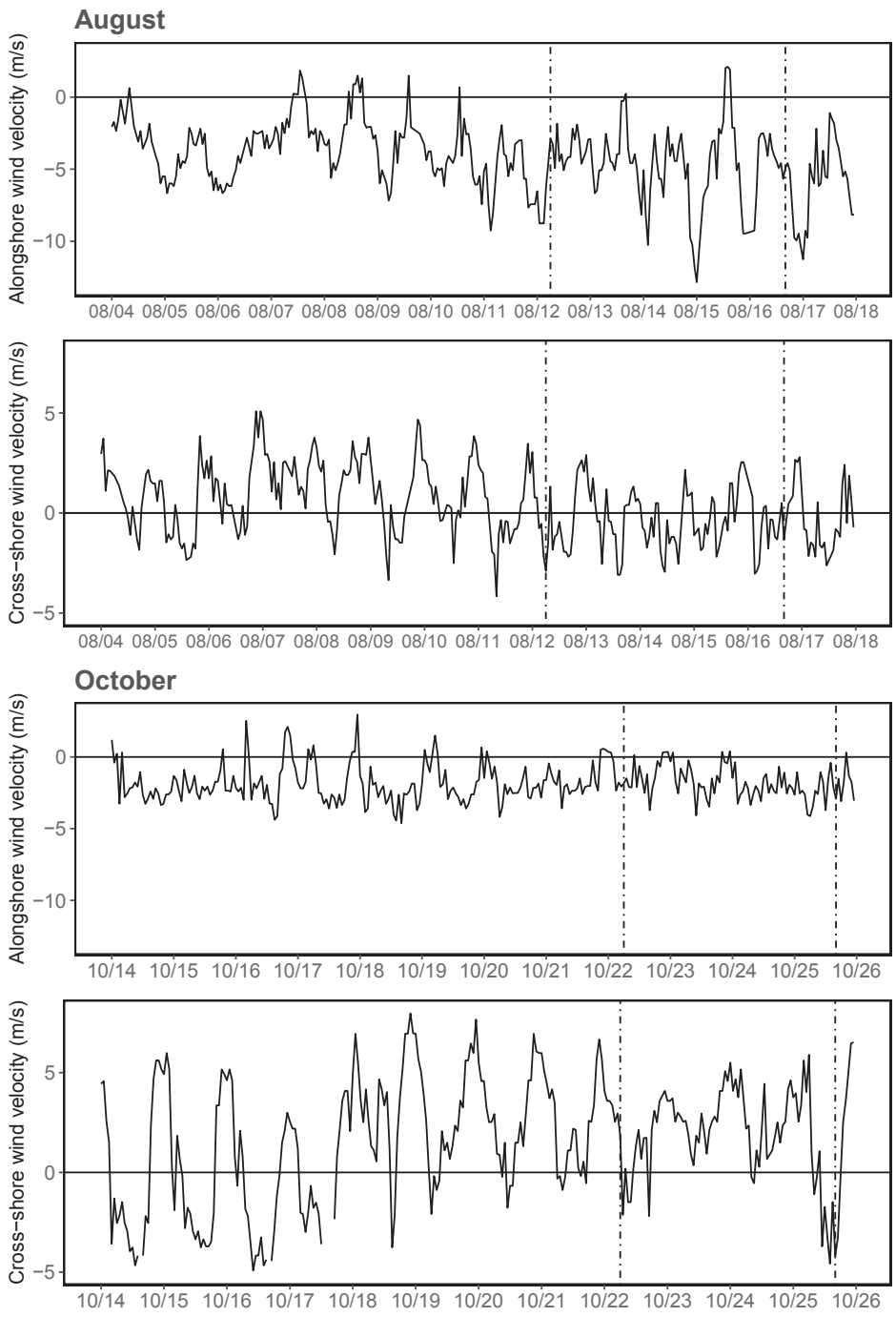

Fig. 4. Hourly variation (Pacific Standard Time) in alongshore and cross-shore wind velocity relative to coastline angle of Monterey Bay (335°) obtained from M1 mooring data (46092) in Monterey Bay for August and October 2013. Positive (+) and negative (−) alongshore wind velocity represent poleward and equatorward winds along the coast, respectively. Positive (+) and negative (−) cross-shore wind velocity represent onshore and offshore winds along the coast, respectively. The start and end of the sampling periods are denoted by the dotted dashed lines, and the zero line is denoted by solid black line. Plots include hourly variation for 8 days prior to each sampling period, since residence times of upwelling shadow water is approximately 8 days (Graham and Largier, 1997) and oceanographic dynamics may have time lags on the order of days.

3.3. Meroplankton assemblage

3.3.1. Composition

Taxonomic groupings consisted of 11 classes or orders, with a variable number of species in each group (Table 1). Anomura consisted of only *Emerita analoga*. Brachyura was comprised of *Metacarcinus (Cancer) magister*, *Romaleon* (*Cancer) antennarius*, *Hemigrapsus nudus*, *Pinnixa faba*, *Pugettia* spp. and *Lophopanopeus bellus*. Cirripedia consisted of *Balanus glandula*, *Balanus crenatus*, *Balanus nubilius*, *Chthamalus dalli*, *Pollicipes polymerus*, and *Semibalanus cariosus*. Echinoidea consisted of *Strongylocentrotus* spp. Gebiidea consisted of only *Upogebia pugettensis*. Gymnolaemata consisted of only *Membranipora membranacea*. Ophiuroidea consisted of predominately *Amphiodia urtica* and Bivalvia mainly consisted of *Kellia suborbicularis* and *Clinocardium nuttallii* (Harvey et al., 2018). Gastropoda mainly consisted of *Amphissa* spp. and *Crepipatella lingulata* and Polychaeta mainly consisted of *Phragmatopoma californica* (Harvey et al., 2018).

In addition, Brachiopoda appeared to be comprised of one predominant stage of lingula larvae (Table 1). Late-stage polychaetes, *Strongylocentrotus* sp., and ophiuroids consisted of recently metamorphosed juveniles; metamorphosis in these taxa often precedes settlement (Strathmann, 1987). Bivalvia, Gastropoda, Cirripedia, Polychaeta, and Gymnolaemata comprised a majority of total individuals in the larval assemblage in both August and October, and Ophiuroidea became a large portion of the larval assemblage in October (Table 1).

Meroplankton assemblages differed significantly between months, with month explaining about 7% of the variation in meroplankton assemblages (PERMANOVA, $F(1,74) = 5.28$, $R^2 = 0.07$, $p < 0.001$;

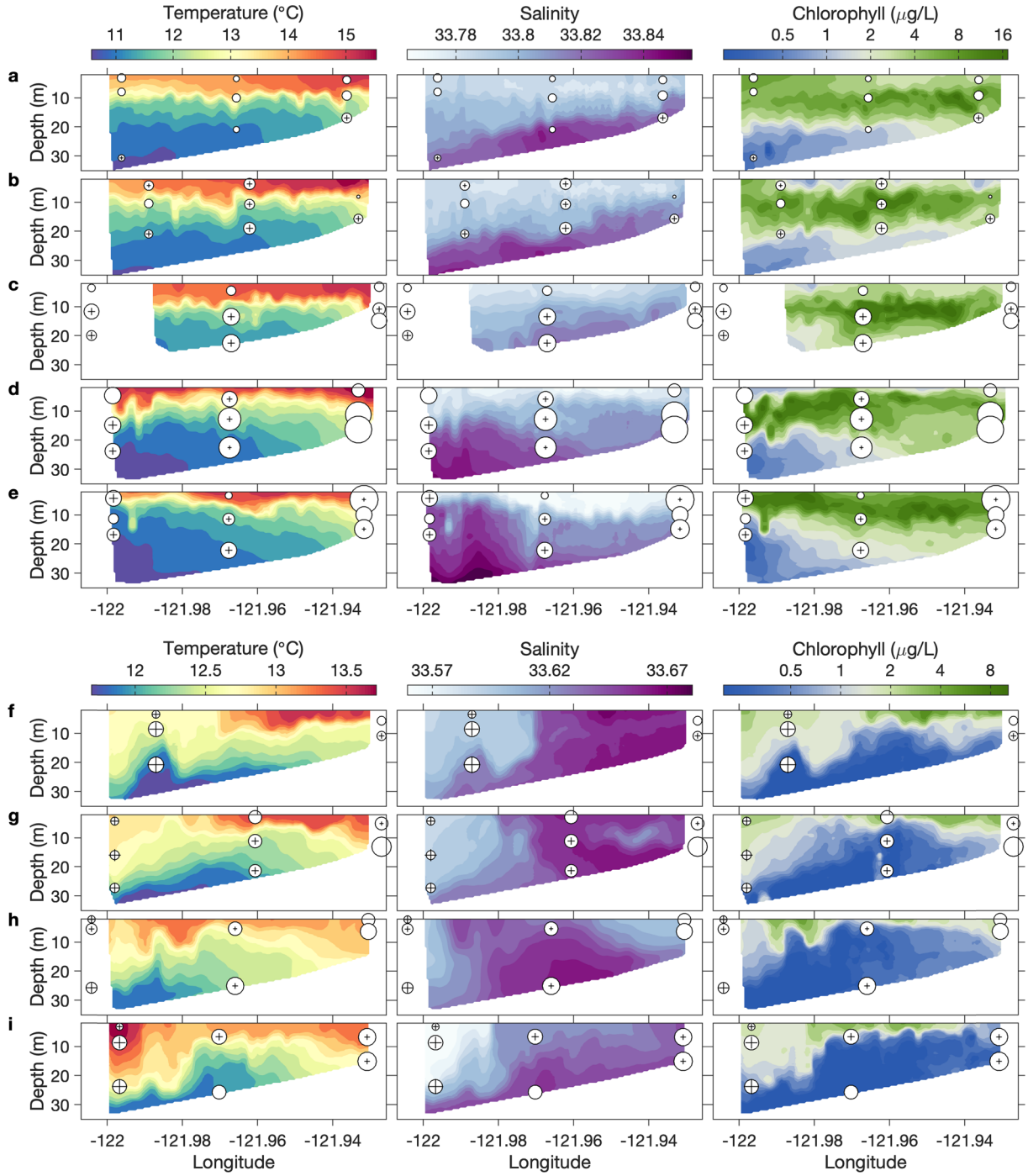

Fig. 5. Daily vertical sections of temperature, salinity, and fluorescence from AUV *Dorado* surveys along the northern Monterey Bay meroplankton sampling transect during 2013, August 12–16 (a-e) and October 22–25 (f-i). Transect endpoints are at the farthest offshore and onshore locations of the ship sampling locations shown in Fig. 1b. White circles and black plus signs indicate larval abundances for nearshore and offshore species, respectively. The scales for the variables depicted are different for August (a-e) and October (f-i) since the range of the variables changed between the two sampling periods.

Fig. 6). The NMDS ordinations revealed fairly high stress levels (2D stress 0.24), indicating weak visual representations of the data in 2-dimensions. The taxa that most influenced differences between months were Bivalvia juveniles (23% contribution to dissimilarity), Polychaeta juveniles (13% contribution to dissimilarity) and trochophores (11% contribution to dissimilarity), Gastropoda juveniles (6% contribution to dissimilarity), and early-stage Ophiuroids (6% contribution to dissimilarity).

Meroplankton assemblages differed significantly between days in August (PERMANOVA, $F(4,39) = 3.39$, $R^2 = 0.26$, $p < 0.001$), but not between days in October (PERMANOVA, $F(3,28) = 18$, $R^2 = 0.11$, $p = 0.26$). Daily fluctuation explained 26% of the variation in larval assemblage between days in August. The NMDS ordinations revealed fairly high stress levels (2D stress August: 0.21 and October: 0.23), indicating weak visual representations of the data reduced to 2-dimensions.

3.3.2. Richness and diversity

Mean taxon richness did not differ between August (8.3 ± 3.2 species) and October (8.96 ± 2.4 species, $t(1,74) = 0.030$, $p = 0.98$). Similarly, Shannon-Weiner diversity did not differ between August (1.4 ± 0.4) and October (1.4 ± 0.3, $t(1,74) = -0.31$, $p = 0.75$).

Table 1
Mean and standard error of larval abundances for each taxonomic group collected in northern Monterey Bay during August and October 2013. Table is ordered by species that tended to be more abundant in August (nearshore group) and October (offshore group). Species of barnacles (Cirripedia) and brachyuran crabs (Brachyura) are included but are grouped for analyses due to their low overall abundances.

			August		October	
Taxon	Stage	Stage name	Mean abundance	Standard error	Mean abundance	Standard error
Nearshore group						
Polychaeta *(Phragmatopoma californica)*	Early	trochophore	83.3	34.7	150.9	54.8
Polychaeta *(Phragmatopoma californica)*	Late	juvenile	86.6	20.1	117.4	23.0
Gastropoda *(Amphissa* spp. & *Crepipatella lingulata)*	Late	veliger	109.0	21.4	13.4	3.0
Bivalvia *(Kellia suborbicularis & Clinocardium nuttallii)*	Late	veliger	515.8	194.0	146.5	30.4
Membranipora membranacea	Early	cyphonautes	83.9	42.9	22.8	4.9
Cirripedia (barnacles)	Early	nauplii	49.4	14.1	9.4	4.0
Cirripedia (barnacles)	Late	cyprid	103.9	79.1	40.6	7.9
Balanus crenatus	Early	nauplii	26.6	9.9	6.3	3.5
Balanus crenatus	Late	cyprid	100.0	78.8	17.2	5.5
Pollicipes polymerus	Early	nauplii	18.4	7.0	1.6	1.0
Pollicipes polymerus	Late	cyprid	0.6	0.3	12.5	3.4
Balanus nubilus	Early	nauplii	2.5	1.5	1.4	1.0
Balanus nubilus	Late	cyprid	0.4	0.2	7.9	1.7
Chthamalus dalli	Early	nauplii	2.0	1.3	0.0	0.0
Chthamalus dalli	Late	cyprid	2.1	1.2	1.8	0.8
Semibalanus cariosus	Late	cyprid	0.7	0.7	0.0	0.0
Balanus glandula	Late	cyprid	0.0	0.0	1.3	0.4
Emerita analoga	Early	zoea	15.4	5.9	1.3	0.8
Brachyura (crabs)	Early	zoea	7.6	2.4	9.2	3.4
Hemigrapsus spp.	Early	zoea	1.1	0.5	0.4	0.3
Pinnotheridae (Pinnixa faba)	Early	zoea	3.5	2.2	6.3	2.9
Lophopanopeus bellus	Early	zoea	0.6	0.4	0.0	0.0
Majidae (Scyra acutifrons)	Early	zoea	0.3	0.2	2.4	1.3
Cancridae	Early	zoea	2.0	0.8	0.2	0.1
Cancridae	Late	megalopa	0.1	0.1	0.0	0.0
Upogebia pugettensis	Early	zoea	0.9	0.7	0.1	0.1
Strongylocentrotus sp.	Early	pluteus	0.5	0.4	0.7	0.5
Strongylocentrotus sp.	Late	juvenile	2.6	1.3	1.2	0.5
Offshore group						
Brachiopoda (Inarticulate)	Early	lingula	1.4	0.5	2.5	1.3
Ophiuroidea *(Amphioida urtica)*	Early	ophiopluteus	5.5	1.9	70.5	33.9
Ophiuroidea *(Amphioida urtica)*	Late	juvenile	1.4	0.5	13.9	5.2

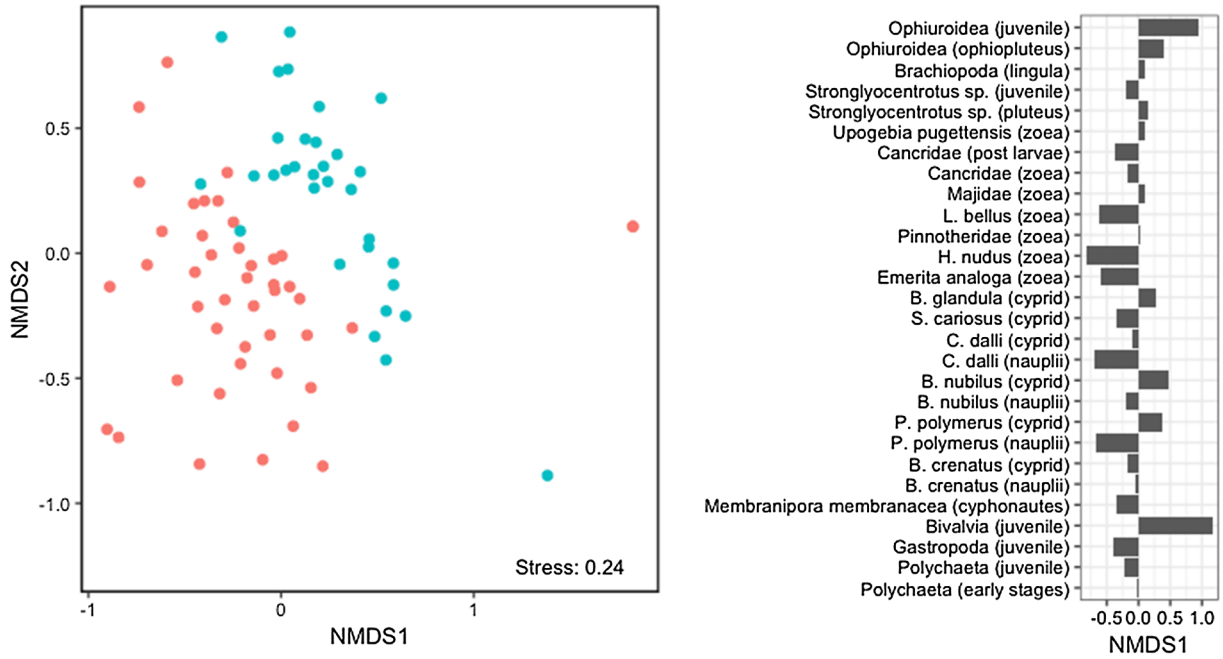

Fig. 6. Nonmetric multidimensional scaling representing larval assemblages in northern Monterey Bay during 2013, August (red circles) and October (blue circles). Stress value is reported in the lower right corner of the plot. Individual taxa scores for NMDS axis 1 are included on the right side of the plot. (For interpretation of the references to colour in this figure legend, the reader is referred to the web version of this article.)

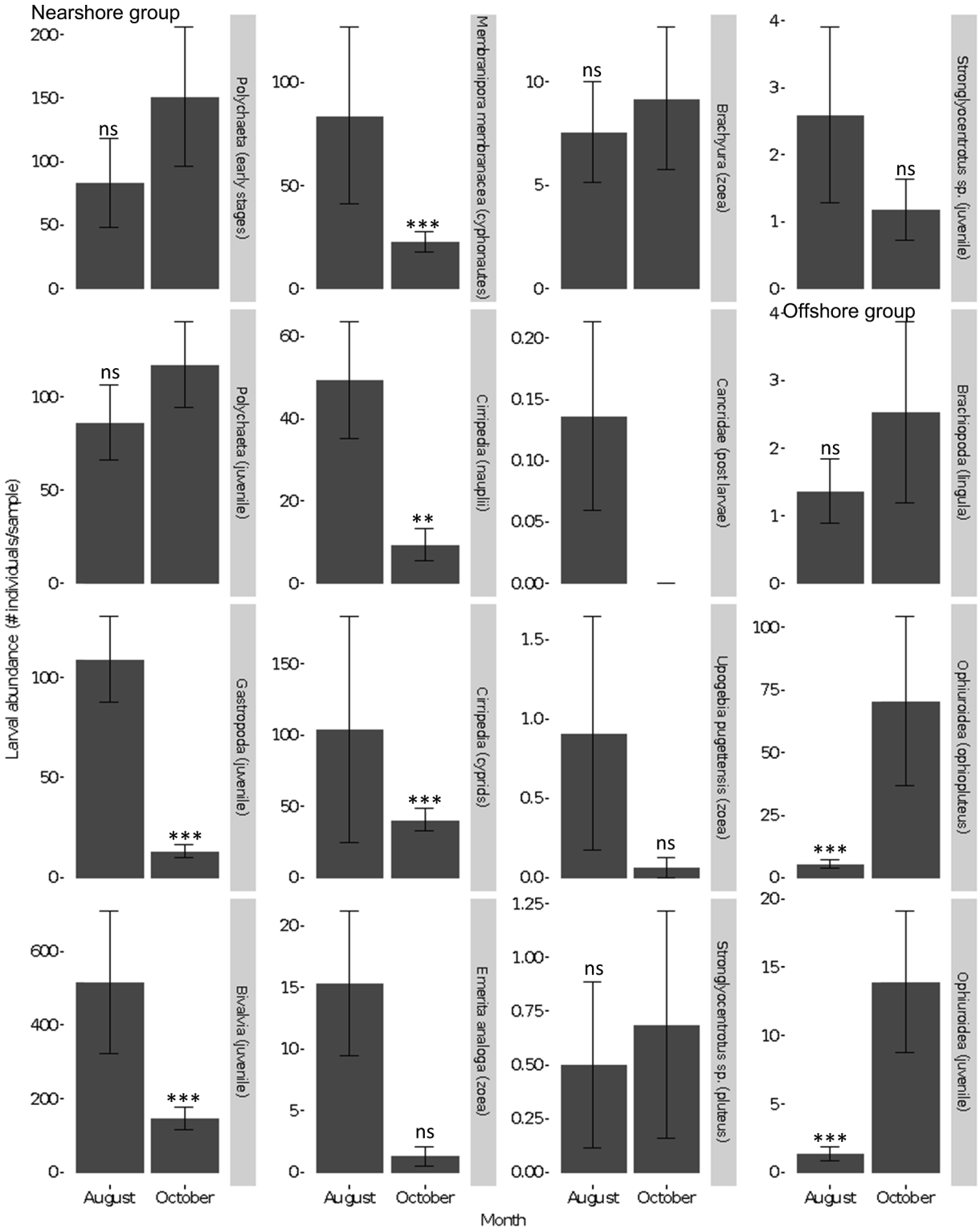

Fig. 7. Mean larval abundances of taxa in northern Monterey Bay during August and October 2013. Values represent means ± SE and are reported in Table 1. Plot grouping indicates taxonomic groups that tended to be more abundant in August (nearshore group) and October (offshore group). Significance values were obtained from zero-inflated negative binomial models to compare differences between months for each taxon and stage combination and are reported in Table 2.

3.4. Larval abundance

3.4.1. Seasonal

Mean abundances of late-stage Gastropoda and Bivalvia larvae, early-stage *Membranipora membranacea* larvae, and early and late-stage Cirripedia larvae were significantly greater in August than October (Fig. 7; Table 2). *Emerita analoga* zoea and *Strongylocentrotus* sp. juveniles also tended to be more abundant in August, although not significantly, and late-stage Cancridae larvae were only collected in August (Fig. 7; Table 2). Conversely, early and late-stage Ophuroidea larvae were significantly more abundant in October (Fig. 7; Table 2).

3.4.2. Daily

Most larval taxa in August followed a trend of peak abundance on

Table 2
Larval abundances of taxa in northern Monterey Bay compared between August and October 2013 (Month) and between days within each month (Day). Significance values (z- and P-values) were computed from zero inflated negative binomial models for each taxonomic group and stage. Significant differences in counts for each taxonomic group are denoted in bold and asterisks (* $p < 0.05$, ** $p < 0.01$, *** $p < 0.001$) and nonsignificant relationships are denoted by ns. Trends (p-value < 0.11) are denoted by ns in italicized font. Superscript plus (+) denotes a significant effect of month or day on the presence or absence of taxa, but not total abundance.

Taxon	Stage	Month		Day	
				August	October
Nearshore group					
Polychaeta *(Phragmatopoma californica)*	Early	ns		***	ns
Polychaeta *(Phragmatopoma californica)*	Late	ns		***	*ns*
Gastropoda *(Amphissa* spp. & *Crepipatella lingulata)*	Late	**August**	***	***	ns
Bivalvia *(Kellia suborbicularis* & *Clinocardium nuttallii)*	Late	**August**	***	(+)***	ns
Membranipora membranacea	Early	**August**	***	***	*
Cirripedia (barnacles)	Early	**August**	**	***	ns
Cirripedia (barnacles)	Late	**August**	***	***	***
Emerita analoga	Early	*August*	*ns*	ns	ns
Brachyura (crabs)	Early	ns		ns	*
Cancridae	Late	August only		ns	*absent*
Upogebia pugettensis	Early	ns		***	–
Strongylocentrotus sp.	Early	ns		–	–
Strongylocentrotus sp.	Late	*August*	*ns*	***	ns
Offshore group					
Brachiopoda (Inarticulate)	Early	–	ns	ns	ns
Ophiuroidea *(Amphioida urtica)*	Early	**October**	***	(+) *ns*	ns
Ophiuroidea *(Amphioida urtica)*	Late	**October**	***	ns	ns

15 Aug 2013 (Bivalvia, Cirripedia, Gastropoda, Gymnolaemata, Polychaeta, Echinoidea- only early stage, Brachyura-only late stage, and Ophiuroidea- only late stage) (Fig. 8). A few taxa, such as Anomura and late stage Echinoidea had different trends in abundance and early stages of Ophiuroidea, Brachiopoda, Gebiidea, and Brachyura were uncommon in August (< 5 individuals) (Fig. 8).

In October, Ophiuroidea, Brachiopoda, and late stage Echinoidea tended to peak on the first day of sampling (22 Oct 2013), decrease on 23 and 24 Oct, and then slightly increase on the last day (Fig. 8). Conversely, Cirripedia (late stage), Gastropoda, Gymnolaemata, Gebiidea, Polychaeta, Echinoidea (early stage), and Brachyura (late stage) tended to be lowest on the first day of sampling (22 Oct 2013) and increase in abundance throughout the sampling period, with a peak on 25 Oct 2013. A few taxa, such Cirripedia (early stage) and Brachyura (early stage) had different trends in abundance and late stage Echinoidea and Anomura were uncommon in October (< 5 individuals) (Fig. 8).

Spearman rank correlations revealed that Gastropoda (juveniles) and *Emerita analoga* (zoea) were most abundant on days with high wind speeds, high salinity, and low minimum temperatures (Table 3). Both stages of Ophiuroids were most abundant on days with lower wind speeds and lower salinity water (Table 3). In addition, Cirripedia nauplii and Gastropoda (juveniles) were most abundant close to the seafloor (Table 3). Lastly, *Emerita analoga* (zoea) were found in higher abundances on days with high average chlorophyll-*a* fluorescence, whereas Ophiuroidea juveniles were found in lower abundances on days with high average chlorophyll-*a* fluorescence (Table 3).

4. Discussion

The composition of the phytoplankton and meroplankton assemblages were influenced by the seasonal oceanographic dynamics in 2013. August was generally characterized by upwelling conditions and October by relaxation conditions, consistent with the oceanographic seasons in Monterey Bay (Pennington and Chavez, 2000). The phytoplankton shifts during our study were related to the observed variation in oceanographic conditions. Interplay between upwelling winds, which caused an upwelling shadow to set up in northern Monterey Bay, and the influx of offshore water from outside the bay were associated with variation in chlorophyll-*a* fluorescence and the phytoplankton assemblage between August and October. Specifically, in August there were much stronger northwesterly winds which may have forced upwelling, causing an upwelling jet to extend southward across the mouth of Monterey Bay, as is characteristic of upwelling conditions (Rosenfeld et al., 1994). In addition, deep, cold, salty water, characteristic of upwelled waters (likely North Pacific deep water) (Warn-Varnas, 2007), occurred throughout August. August consisted of strong thermal stratification, with relatively warm surface waters inshore in the northeastern corner of Monterey Bay caused by solar heating, which signifies the presence of an upwelling shadow (Graham and Largier, 1997). Chlorophyll-*a* is a proxy for phytoplankton abundance and larval food supply, depending on the species composition of the phytoplankton assemblage (Wilkerson et al., 2000, Vargas et al., 2006). Higher chlorophyll-*a* in August may have resulted from higher productivity in response to greater upwelling and nutrient delivery (Pennington and Chavez, 2000), greater retention and associated accumulation of phytoplankton biomass in the upwelling shadow (Graham and Largier, 1997; Ryan et al., 2017), or variation in phytoplankton community composition between sampling periods (Lassiter et al., 2006). The influx of low salinity, offshore water into the study domain in October may have also contributed to seasonal chlorophyll-*a* differences, because California Current waters are relatively chlorophyll-poor compared to nearshore waters.

The phytoplankton community composition, at least at the Santa Cruz Wharf monitoring site, shifted from August to October. The dominant phytoplankton species in August consisted of diatoms, namely *Pseudo-nitzschia* spp., but shifted to dinoflagellates (*Cochlodinium* and *Ceratium*) in October. The shift from a diatom to dinoflagellate dominated phytoplankton community tracks the characteristic seasonal variability in Monterey Bay. Diatoms, including *Pseudo-nitzchia* spp., are most abundant in spring and summer when upwelling is highest (Kudela et al., 2005). The influx of offshore water and associated decrease in nutrient concentrations during fall tends to favor dinoflagellates, because they are capable of migrating vertically in the water column to access the sunlight at the surface and nutrients in the thermocline (Kudela et al., 2008; Ryan et al., 2008, 2010). In addition, these results are consistent with Bolin and Abbott (1963) who found high relative abundances of *Ceratium* with the influx of waters from outside of the bay, often in fall (peak relative abundances around October).

Meroplankton assemblages appeared to be similarly affected by upwelling and relaxation dynamics in Monterey Bay, through the interplay between the upwelling shadow and upwelled water in August and weaker upwelling winds which led to greater influx of offshore water in October. The stabilizing effect of the upwelling shadow on larval assemblages was reflected in the average diversity and richness of the larval assemblages. Larval richness and diversity did not differ significantly between sampling periods, suggesting that similar taxa were present and reproducing throughout both August and October.

Although larval species richness and diversity did not differ substantially between months, species level differences were detected between August and October (Fig. 6; Fig. 7; Table 2). Differing seasonal oceanographic conditions, leading to differing water mass histories between the two sampling periods, may have contributed to this difference. In August, the meroplankton assemblage in the stratified, nearshore waters of the upwelling shadow retention zone was characterized by more coastal, nearshore species, and offshore species were present in the cold, salty upwelled water (Fig. 5a-e). Taxonomic groups

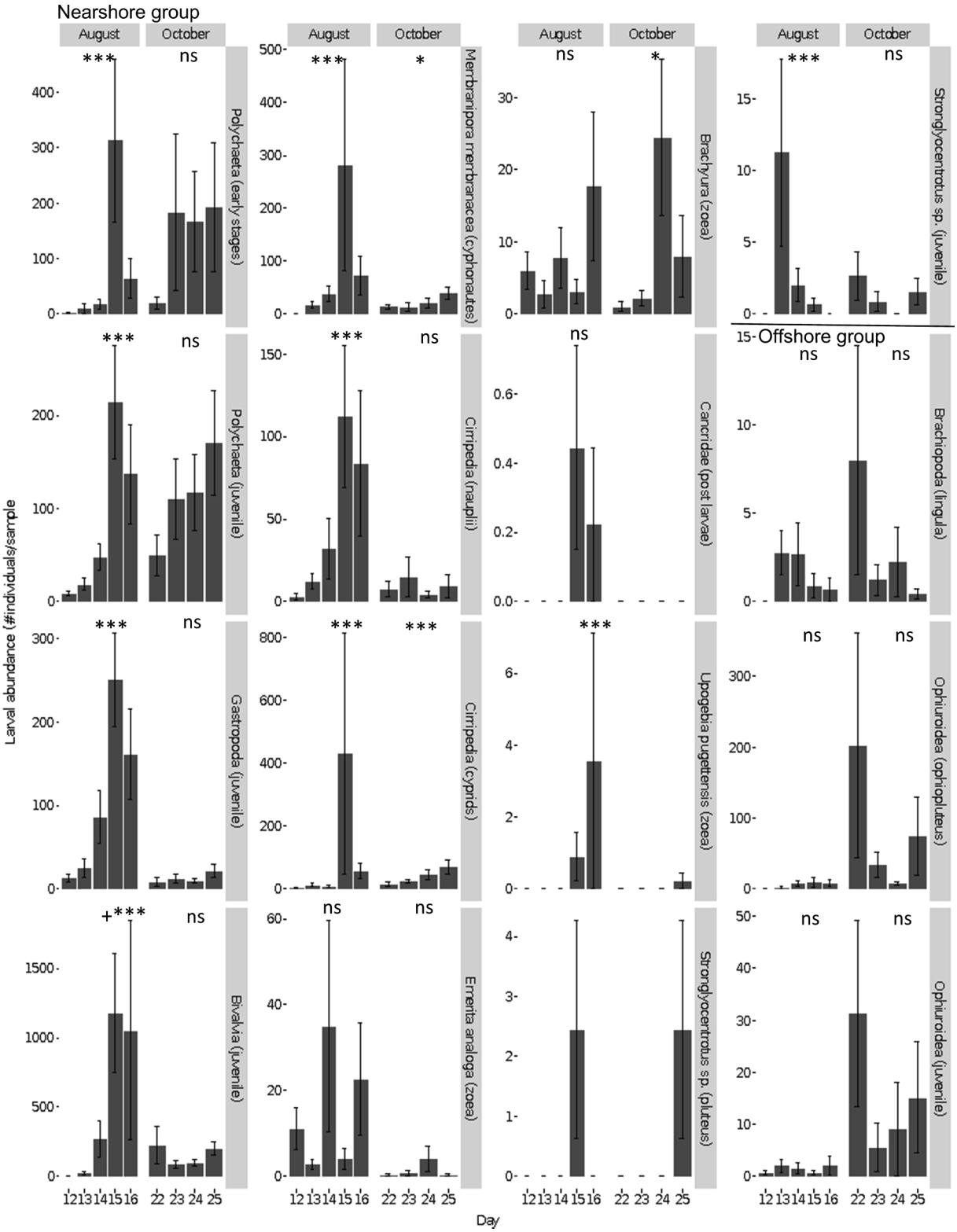

Fig. 8. Mean daily larval abundances of taxa collected in northern Monterey Bay during August and October 2013. Plot grouping indicates taxonomic groups that tended to be more abundant in August (nearshore group) and October (offshore group) and with similar patterns in both months. Values represent means ± SE. Significance values were obtained from zero-inflated negative binomial models to compare differences between days in each month for each taxon and stage combination and are reported in Table 2.

that tended to be more abundant in August included *E. analoga* (Anomura) that are restricted to sandy beach intertidal zones, barnacles (Cirripedia) that live attached to rocks and other substrata nearshore, gastropods and clams that occur mainly in shallow estuarine habitats, and *M. membranacea* (Gymnolaemata), a bryozoan that inhabits shallow water (Fig. 7; Table 2).

Larvae of many nearshore species were still retained nearshore in October, but the assemblage contained much higher abundances of

Table 3
Spearman rank correlation coefficients between daily environmental variables (mean, median, maximum, minimum) and total daily larval abundances of each taxa. Significant correlations are denoted in bold and asterisks (* $p < 0.05$, ** $p < 0.01$, *** $p < 0.001$) and nonsignificant relationships are denoted by ns. Trends (p-value < 0.11) are denoted by ns in italicized font.

		Polychaeta (trochophore)		Polychaeta (juvenile)		Gastropoda (juvenile)		Bivalvia (juvenile)		*Membranipora membranacea* (cyphonautes)		Cirripedia (nauplii)		Cirripedia (cyprids)		*Emerita analoga* (zoea)
Wind Speed																
	mean	−0.20	ns	−0.03	ns	**0.72**	*	0.28	ns	0.38	ns	0.30	ns	−0.07	ns	**0.73**
	max	0.02	ns	0.22	ns	**0.81**	**	*0.64*	*ns*	*0.63*	*ns*	0.54	ns	0.14	ns	0.58
	min	−0.52	ns	−0.37	ns	0.39	ns	−0.15	ns	0.00	ns	−0.07	ns	−0.37	ns	**0.79**
Wind Dir																
	median	−0.31	ns	−0.18	ns	**0.68**	*	0.11	ns	0.25	ns	0.21	ns	−0.18	ns	0.53
Relative wind speed																
Alongshore																
	mean	0.17	ns	0.07	ns	**−0.77**	*	−0.15	ns	−0.33	ns	−0.33	ns	0.08	ns	*−0.60*
	median	0.36	ns	0.23	ns	0.64	*ns*	−0.02	ns	−0.20	ns	−0.13	ns	0.23	ns	−0.57
	max	0.23	ns	0.33	ns	−0.28	ns	0.45	ns	0.15	ns	0.10	ns	0.27	ns	0.05
	min	0.00	ns	−0.13	ns	**−0.93**	***	−0.45	ns	−0.55	ns	**−0.66**	*	−0.08	ns	**−0.68**
Cross-shore																
	mean	0.26	ns	0.11	ns	**−0.77**	*	−0.50	ns	−0.38	ns	*−0.60*	*ns*	0.17	ns	**−0.70**
	median	0.28	ns	0.21	ns	**−0.68**	*	−0.30	ns	−0.20	ns	−0.48	ns	0.25	ns	*−0.57*
	max	0.13	ns	0.03	ns	**−0.85**	**	−0.38	ns	−0.43	ns	**−0.70**	*	0.08	ns	**−0.79**
	min	0.05	ns	−0.07	ns	*−0.61*	*ns*	−0.21	ns	−0.39	ns	−0.30	ns	−0.01	ns	−0.25
Salinity																
	mean	−0.15	ns	−0.08	ns	**0.77**	*	0.23	ns	0.23	ns	0.50	ns	−0.12	ns	*0.60*
	max	−0.18	ns	−0.08	ns	**0.68**	*	0.22	ns	0.20	ns	0.45	ns	−0.10	ns	**0.74**
	min	−0.38	ns	−0.32	ns	*0.60*	*ns*	−0.03	ns	0.03	ns	0.38	ns	−0.25	ns	0.45
Temperature																
	mean	−0.47	ns	−0.23	ns	*0.65*	*ns*	0.13	ns	0.20	ns	0.35	ns	−0.18	ns	0.48
	max	−0.12	ns	0.12	ns	**0.88**	**	0.53	ns	0.55	ns	*0.63*	*ns*	0.08	ns	*0.63*
	min	0.35	ns	0.12	ns	**−0.70**	*	−0.18	ns	−0.32	ns	−0.30	ns	0.15	ns	**−0.87**
Oxygen																
	mean	0.10	ns	0.20	ns	−0.55	ns	−0.05	ns	−0.12	ns	−0.48	ns	0.23	ns	−0.52
	max	0.48	ns	0.52	ns	0.53	ns	0.45	ns	0.47	ns	**0.75**	*	0.50	ns	−0.04
	min	0.00	ns	0.03	ns	−0.40	ns	0.03	ns	0.07	ns	−0.43	ns	0.05	ns	−0.49
Distance above seafloor																
	mean	−0.22	ns	−0.18	ns	**−0.78**	*	−0.40	ns	−0.40	ns	**−0.83**	**	−0.13	ns	−0.49
	max	−0.31	ns	−0.31	ns	**−0.78**	*	−0.29	ns	−0.49	ns	**−0.82**	**	−0.36	ns	−0.17
	min	−0.41	ns	*−0.62*	*ns*	**−0.77**	*	−0.46	ns	**−0.82**	**	−0.45	ns	*−0.62*	*ns*	−0.24
Chlorophyll-*a*																
	mean	−0.43	ns	−0.33	ns	0.53	ns	0.15	ns	0.02	ns	0.27	ns	−0.37	ns	**0.70**
	max	−0.30	ns	−0.40	ns	0.20	ns	−0.03	ns	−0.30	ns	0.13	ns	−0.45	ns	0.42
	min	−0.30	ns	−0.23	ns	0.20	ns	0.22	ns	0.00	ns	0.13	ns	−0.20	ns	−0.03

	Emerita analoga (zoea)	Brachyura (zoea)		Cancridae (post larvae)		*Upogebia pugettensis* (zoea)		*Strongylo-centrotus* sp. (pluteus)		*Strongylo-centrotus* sp. (juvenile)		Brachiopoda (lingula)		Ophiuroidea (ophiopluteus)		Ophiuroidea (juvenile)	
Wind Speed																	
	*	0.28	ns	0.55	ns	0.33	ns	0.21	ns	−0.34	ns	−0.35	ns	*−0.62*	*ns*	**−0.89**	**
	ns	0.23	ns	*0.64*	*ns*	0.58	ns	0.42	ns	−0.14	ns	−0.33	ns	−0.21	ns	**−0.67**	*
	*	0.37	ns	0.23	ns	−0.01	ns	−0.23	ns	−0.47	ns	−0.30	ns	**−0.89**	**	**−0.80**	**
Wind Dir																	
	ns	0.08	ns	0.40	ns	0.25	ns	0.26	ns	−0.10	ns	−0.33	ns	*−0.62*	*ns*	**−0.86**	**

(*continued on next page*)

Table 3 (*continued*)

	Emerita analoga (zoea)		Brachyura (zoea)		Cancridae (post larvae)		*Upogebia pugettensis* (zoea)		*Strongylo-centrotus* sp. (pluteus)		*Strongylo-centrotus* sp. (juvenile)		Brachiopoda (lingula)		Ophiuroidea (ophiopluteus)		Ophiuroidea (juvenile)	
Relative wind speed Alongshore																		
	ns		−0.18	ns	−0.46	ns	−0.29	ns	−0.31	ns	0.20	ns	0.4	ns	*0.633*	*ns*	**0.92**	***
	ns		−0.16	ns	−0.34	ns	−0.20	ns	−0.21	ns	0.17	ns	0.377	ns	**0.695**	*	**0.86**	**
	ns		0.22	ns	0.14	ns	0.19	ns	−0.31	ns	−0.25	ns	0.183	ns	0.517	ns	0.53	ns
	*		−0.21	ns	*−0.64*	*ns*	−0.50	ns	−0.31	ns	0.19	ns	0.36	ns	0.43	ns	**0.87**	**
Cross-shore																		
	*		0.04	ns	−0.53	ns	−0.31	ns	−0.05	ns	−0.04	ns	0.059	ns	0.36	ns	**0.76**	*
	ns		0.25	ns	−0.46	ns	−0.15	ns	−0.10	ns	−0.10	ns	0.033	ns	0.433	ns	**0.85**	**
	*		−0.17	ns	−0.52	ns	−0.28	ns	0.00	ns	0.10	ns	0.083	ns	0.55	ns	**0.84**	**
	ns		−0.34	ns	−0.12	ns	−0.45	ns	−0.36	ns	−0.04	ns	0.51	ns	0.15	ns	0.49	ns
Salinity																		
	ns		−0.07	ns	0.55	ns	0.33	ns	0.21	ns	−0.19	ns	−0.40	ns	−0.47	ns	**−0.94**	***
	*		0.03	ns	*0.64*	*ns*	0.30	ns	0.00	ns	−0.41	ns	−0.33	ns	−0.57	ns	**−0.95**	***
	ns		−0.28	ns	0.43	ns	0.10	ns	−0.10	ns	0.05	ns	0.00	ns	*−0.60*	*ns*	**−0.79**	*
Temperature																		
	ns		−0.03	ns	0.48	ns	0.39	ns	−0.10	ns	0.00	ns	−0.17	ns	−0.47	ns	*−0.59*	*ns*
	ns		0.17	ns	**0.71**	*	*0.63*	*ns*	0.21	ns	−0.15	ns	−0.33	ns	−0.30	ns	**−0.71**	*
	**		−0.50	ns	−0.48	ns	−0.39	ns	0.10	ns	0.49	ns	0.47	ns	**0.70**	*	**0.79**	*
Oxygen																		
	ns		0.10	ns	−0.16	ns	0.16	ns	0.00	ns	−0.12	ns	−0.12	ns	0.55	ns	**0.75**	*
	ns		0.00	ns	0.48	ns	*0.66*	*ns*	0.31	ns	0.00	ns	−0.30	ns	0.40	ns	−0.03	ns
	ns		0.00	ns	−0.39	ns	−0.21	ns	0.21	ns	0.49	ns	0.45	ns	0.32	ns	*0.61*	*ns*
Distance above seafloor																		
	ns		0.07	ns	−0.55	ns	−0.33	ns	−0.21	ns	0.05	ns	0.15	ns	0.22	ns	**0.72**	*
	ns		0.10	ns	−0.60	ns	−0.45	ns	−0.31	ns	−0.09	ns	0.06	ns	0.14	ns	0.51	ns
	ns		*−0.63*	*ns*	*−0.66*	*ns*	**−0.85**	**	*−0.66*	*ns*	0.38	ns	*0.62*	*ns*	0.09	ns	0.36	ns
Chlorophyll-*a*																		
	*		−0.13	ns	0.43	ns	0.10	ns	−0.10	ns	−0.20	ns	−0.20	ns	−0.57	ns	**−0.89**	**
	ns		−0.47	ns	0.16	ns	−0.23	ns	−0.10	ns	−0.07	ns	−0.08	ns	−0.35	ns	**−0.74**	*
	ns		*−0.62*	*ns*	0.25	ns	0.02	ns	0.10	ns	0.46	ns	0.32	ns	0.02	ns	−0.26	ns

widespread, shelf species, transported into the sampling domain by the persistent influx of offshore water (Fig. 5f-i). The primary taxon that became more abundant in October was Ophiuroidea (Fig. 7; Table 2), mainly *A. urtica,* a widespread brittle star that inhabits soft sediment regions of the shelf (Bergen et al., 2001). Brachiopoda, which tend to be found in deep, soft sediment habitats in Monterey Bay (Pennington et al., 1999), showed a similar trend, although their numbers were too low to detect significant differences (Fig. 7; Table 2). These characteristic shelf species were present predominantly in the fresher, offshore water type in October (Fig. 5f-i).

The observed taxonomic changes between months did not appear to be strongly influenced by differences in reproductive seasons because both early and late-stage larvae of nearly all taxa were detected during both months (Table 1). In addition, many species that varied significantly between months (e.g., *A. urtica*, *E. analoga*) have reproductive seasons that span both sampling periods (*A. urtica*— all year; Thompson and Bergen, 1993, *E. analoga*—April to October; Boolootian et al., 1959). Rather, the observed differences in larval assemblages likely resulted from changing source waters to Monterey Bay and the associated differences in oceanographic conditions. In August, nearshore retention in the upwelling shadow was stronger, whereas flushing of the upwelling shadow region with offshore, low-salinity water occurred in October. This is consistent with greater overall abundances of nearshore, coastal species in August, and conversely, relatively greater abundances of geographically widespread shelf taxa in October (Fig. 7; Table 2). In fact, the northward flows immediately preceding October sampling were the strongest recorded at M1 during 2013 (Fig. 2d). These northward velocity anomalies extended deeper than 100 m and were followed by strong onshore flow (Fig. 2e), which likely transported larvae from the shelf and upper slope south of the bay, into Monterey Bay. Additionally, the seafloor south of Monterey Bay consists mostly of fine to medium grain sediment (< 100 m depth) and the shelf is much narrower, which is consistent with the greater larval abundances of predominately softer sediment, shelf species observed in October (Johnson et al., 2016).

Daily variations in larval abundances were only detected in August, with most of the abundant nearshore species having significantly higher abundances on 15 August 2013 (Fig. 8). This may be related to the increase in upwelling favorable conditions on August 15th, evidenced by the cool, salty water offshore (Fig. 5d-e) and the strong southward winds (Fig. 4), which may increase water movement and the transport of species into the bay. In support of this, a few of the taxa that were found in significantly higher abundances in the August upwelling period (Table 2), namely Gastropoda (juveniles) and *Emerita analoga* (zoea), were also most abundant on days with upwelling favorable conditions, characterized by high wind speeds, high salinity, and low minimum temperatures (Table 3). Similarly, barnacle nauplii (Cirripedia) were found on days with strong upwelling favorable winds (Table 3). This indicates that larvae of these taxa may be transported into the study area during periods of strong upwelling. Most of the other abundant nearshore taxa, except polychaetes, showed a similar, although non-significant, pattern in fluctuation of daily abundances in relation to wind conditions (Table 3). Patterns between daily environmental conditions and larval abundances for certain taxa and stages may not be detectable since many planktonic marine larvae, especially later stages, can vertically migrate in the water column (Morgan and Fisher, 2010).

In October, larval abundances of most taxa did not vary significantly between days, which may be related to the consistent onshore movement of water throughout the sampling period (Fig. 2e), so fresher, offshore water was present in the sampling domain for all sampling days (Fig. 5f-i). Even though larval abundances did not differ significantly for most taxa between days in October, offshore species tended to be present in the offshore water mass each day (Fig. 5f-i). In support of this, ophiuroids were most abundant on days with lower wind speeds and lower salinity water, suggesting that they may be transported into the study region during periods of relaxation (Table 3). Nearshore taxa, such as barnacle cyprids (Cirripedia), *M. membranacea*, and Brachyura, became increasingly more abundant throughout the October sampling period and were found in samples close to the seafloor (Fig. 8; Table 2; Table 3).

The abundance and composition of the larval assemblage in northern Monterey Bay varied with upwelling and relaxation dynamics. Larvae of nearshore species were retained in the recirculation feature that formed in the lee of the headland during upwelling in the summer, and larvae were transported into the northern bay from offshore when alongshore winds relaxed and cross-shore winds increased. Larval assemblages can serve as clear indicators of water mass history (e.g., nearshore versus offshore). On the other hand, knowledge of water types can provide insight into the diversity and abundance characteristics of the nearshore larval supply during changing oceanographic conditions, and therefore inform predictions about subsequent settlement and recruitment. Overall, the highly variable nature of circulation in nearshore upwelling regions, due to variable wind forcing, makes predicting circulation, larval supply, and the resulting recruitment challenging. However, relationships between larval taxa, including life history stage characteristics, and seasonal variation in source water types can provide a valuable indication of differences in water mass history and circulation in highly dynamic upwelling regions. The results of this study should be applicable to other upwelling regions with prominent bays and coastal promontories.

Acknowledgements

We thank S. Bashevkin, C. Dibble, H. Killeen, E. Kiskaddon, A. Shain, and M. Minton for laboratory assistance. This research was supported by the National Science Foundation Graduate Research Fellowship (1650042) and the David and Lucile Packard Foundation (MBARI project #901026). We would like to thank the captain and crew of the R/V Rachel Carson, the Dorado AUV operations team, M. Salisbury, and the R. Vrijenhoek lab (MBARI) for logistical support. In addition, we would like to thank the Ocean Data Center and Raphael Kudela Lab at University of California, Santa Cruz for phytoplankton data.

References

Bartilotti, C., Santos, A. Dos, Castro, M., Peliz, Alvaro, Santos, A.M.P., 2014. Decapod larval retention within distributional bands in a coastal upwelling ecosystem. Mar. Ecol. Prog. Ser. 507, 233–247.

Bergen, M., Weisberg, S.B., Smith, R.W., Cadien, D.B., Dalkey, A., Montagne, D.E., et al., 2001. Relationship between depth, sediment, latitude, and the structure of benthic infaunal assemblages on the mainland shelf of southern California. Mar. Biol. 138, 637–647.

Bolin, R.L., Abbott, D.P., 1963. Studies on the marine climate and phytoplankton of the central coastal area of California, 1954–1960. California Cooperat. Oceanic Fisheries Investigat. 9, 23–45.

Boolootian, R.A., Giese, A.C., Parmanfarmalan, A., Tucker, J., 1959. Reproductive cycles of five west coast crabs. Physiol. Zoölogy 32, 213–220.

Campbell, J.W., 1995. The lognormal distribution as a model for bio-optical variability in the sea. J. Geophys. Res. Oceans 100 (C7), 13237–13254.

Clarke, K.R., Warwick, R.M., 2001. Change in marine communities: an approach to statistical analysis and interpretation, 2nd ed. Prim. Plymouth UK, pp. 172.

Fisher, J.L., Peterson, W.T., Morgan, S.G., 2014. Does larval advection explain latitudinal differences in recruitment across upwelling regimes? Mar. Ecol. Prog. Ser. 503, 123–137.

Gan, J., Allen, J.S., 2002. A modeling study of shelf circulation off northern California in the region of the Coastal Ocean Dynamics Experiment 2. Simulations and comparisons with observations. J. Geophys. Res. 107 (C11), 3184.

Graham, W.M., Field, J.G., Potts, D.C., 1992. Persistent “upwelling shadows” and their influence on zooplankton distributions. Mar. Biol. 114, 561–570.

Graham, W.M., Largier, J.L., 1997. Upwelling shadows as nearshore retention sites: The example of northern Monterey Bay. Cont. Shelf Res. 17, 509–532.

Harvey, J.B.J., Ryan, Marin III, R., Preston, C.M., Alvarado, N., Scholin, C.A., Vrijenhoek, R.C., 2012. Robotic sampling, in situ monitoring and molecular detection of marine zooplankton. J. Exp. Mar. Biol. Ecol. 413, 60–70.

Harvey, J.B.J., Fisher, J.L., Ryan, J.P., Johnson, S.B., Peterson, W.T., Vrijenhoek, R.C., 2018. Changes in zooplankton assemblages in northern Monterey Bay, California, during a fall transition. Mar Ecol Prog Ser 604, 99–120.

Hickey, B., 1998. Coastal oceanography of Western North America from the tip of Baja California to Vancouver Island. In: Robinson, A., Brink, K.H. (Eds.), The Sea: Ideas and Observations on Progress in the Study of the Seas. John Wiley & Sons, New York, pp. 10339–10368.

Huyer, A., 1983. Coastal upwelling in the California current system. Prog. Oceanogr. 12, 259–284.

Johnson, S.Y., Dartnell, P., Hartwell, S.R., Cochrane, G.R., Golden, N.E., Watt, J.T., Davenport, C.W., Kvitek, R.G., Erdey, M.D., Krigsman, L.M., Sliter, R.W., Maier, K.L., 2016. California State Waters Map Series—Offshore of Monterey, California: U.S. Geological Survey Open-File Report 2016–1110, vol. 44, pp. 1–10.

Jester, R., Lefebvre, K., Langlois, G., Vigilant, V., Baugh, K., Baugh, M.W., 2009. A shift in the dominant toxin-producing algal species in central California alters phycotoxins in food webs. Harmful Algae 8, 291–298. https://doi.org/10.1016/j.hal.2008.07.001.

Kudela, R.M., Pitcher, G., Probyn, T., Figueiras, F., Moita, T., Trainer, V., 2005. Harmful algal blooms in coastal upwelling systems. Oceanography 18, 184–197.

Kudela, R.M., Ryan, J.P., Blakely, M.D., Lane, J.Q., Peterson, T.D., 2008. Linking the physiology and ecology of Cochlodinium to better understand harmful algal bloom events: A comparative approach. Harmful Algae 7, 278–292.

Largier, J.L., Magnell, B.A., Winant, C.D., 1993. Subtidal circulation over the northern California shelf. J. Geophys. Res. 98 (C10), 18147–18179.

Lassiter, A.M., Wilkerson, F.P., Dugdale, R.C., Hogue, V.E., 2006. Phytoplankton assemblages in the CoOP-WEST coastalupwelling area. Deep-Sea Res II 53, 3063–3077.

Levin, L.A., 2006. Recent progress in understanding larval dispersal: new directions and digressions. Integr. Comp. Biol. 46, 282–297.

Mace, A.J., Morgan, S.G., 2006. Biological and physical coupling in the lee of a small headland: Contrasting larval transport mechanisms in an upwelling region, 324, 185–196.

Martin, T.G., Wintle, B.A., Rhodes, J.R., Kuhnert, P.M., Field, S.A., Low-Choy, S.J., et al., 2005. Zero tolerance ecology: Improving ecological inference by modelling the source of zero observations. Ecol. Lett. 8, 1235–1246.

Morgan, S.G., Fisher, J.L., Miller, S.H., McAfee, S.T., Largier, J.L., 2009. Nearshore larval retention in a region of strong upwelling and recruitment limitation. Ecology 90, 3489–3502.

Morgan, S., Fisher, J., 2010. Larval behavior regulates nearshore retention and offshore migration in an upwelling shadow and along the open coast. Mar. Ecol. Prog. Ser. 404, 109–126.

Morgan, S.G., Fisher, J.L., Largier, J.L., 2011. Larval retention, entrainment, and accumulation in the lee of a small headland: Recruitment hotspots along windy coasts. Limnol. Oceanogr. 56, 161–178.

Morgan, S.G., 2014. Behaviorally Mediated Larval Transport in Upwelling Systems.

Oksanen, Jari, F. Guillaume Blanchet, Michael Friendly, Roeland Kindt, Pierre Legendre, Dan McGlinn, Peter R. Minchin, R.B. O'Hara, Gavin L. Simpson, Peter Solymos, M. Henry H. Stevens, Eduard Szoecs and Helene Wagner, 2016. Vegan: Community Ecology Package. R package version 2.4-0.

Pennington, J.T., Tamburri, M.N., Barry, J.P., 1999. Development, temperature tolerance, and settlement preference of embryos and larvae of the articulate brachiopod Laqueus californianus. Biol. Bull. 196, 245–256.

Pennington, T.J., Chavez, F.P., 2000. Seasonal fluctuations of temperature, salinity, nitrate, chlorophyll and primary production at station H3/M1 over 1989–1996 in Monterey Bay, California. Deep Res. Part II Top. Stud. Oceanogr. 47, 947–973.

Pineda, J., Hare, J., Sponaugle, S., 2007. Larval transport and dispersal in the coastal ocean and consequences for population connectivity. Oceanography 20, 22–39.

R Core Team, 2017. R: A language and environment for statistical computing. R Foundation for Statistical Computing, Vienna, Austria.

Ramp, S.R., Paduan, J.D., Shulman, I., Kindle, J., Bahr, F.L., Chavez, F., 2005. Observations of upwelling and relaxation events in the northern Monterey Bay during August 2000. J. Geophys. Res. C Ocean. 110, 1–21.

Rosenfeld, L.K., Schwing, F.B., Garfield, N., Tracy, D.E., 1994. Bifurcated flow from an upwelling center: a cold water source for Monterey Bay. Cont. Shelf Res. 14.

Ryan, J.P., Gower, J.F.R., King, S.A., Bissett, W.P., Fischer, A.M., Kudela, R.M., et al., 2008. A coastal ocean extreme bloom incubator. Geophys. Res. Lett. 35, 4–8.

Roughan, M., Mace, A., Largier, J., Morgan, S., Fisher, J., Carter, M., 2005. Subsurface recirculation and larval retention in the lee of a small headland: A variation on the upwelling shadow theme. J. Geophys. Res. C: Oceans 110 (C10), 1–18. https://doi.org/10.1029/2005JC002898.

Ryan, J.P., Fischer, A.M., Kudela, R.M., Gower, J.F.R., King, S.A., Marin, R., et al., 2009. Influences of upwelling and downwelling winds on red tide bloom dynamics in Monterey Bay, California. Cont. Shelf Res. 29, 785–795.

Ryan, J.P., McManus, M.A., Sullivan, J.M., 2010. Interacting physical, chemical and biological forcing of phytoplankton thin-layer variability in Monterey Bay, California. Continent. Shelf Res. 30, 7–16.

Ryan, J.P., Harvey, J.B.J., Zhang, Y., Woodson, C.B., 2014a. Distributions of invertebrate larvae and phytoplankton in a coastal upwelling system retention zone and peripheral front. J. Exp. Mar. Bio. Ecol. 459, 51–60.

Ryan, J.P., McManus, M.A., Kudela, R.M., Lara Artigas, M., Bellingham, J.G., Chavez, F.P., Doucette, G., Foley, D., Godin, M., Harvey, J.B.J., Marin III, R., Messié, M., Mikulski, C., Pennington, T., Py, F., Rajan, K., Shulman, I., Wang, Z., Zhang, Y., 2014b. Boundary influences on HAB phytoplankton ecology in a stratification-enhanced upwelling shadow. Deep Sea Res. II 101, 63–79. https://doi.org/10.1016/j.dsr2.2013.0017.

Ryan, J.P., Kudela, R.M., Birch, J.M., Blum, M., Bowers, H.A., Chavez, F.P., Doucette, G.J., Hayashi, K., Marin III, R., Mikulski, C.M., Pennington, J.T., Scholin, C.A., Smith, G.J., Woods, A., Zhang, Y., 2017. Causality of an extreme harmful algal bloom in Monterey Bay, California, during the 2014–2016 northeast Pacific warm anomaly. Geophys. Res. Lett. 44. https://doi.org/10.1002/2017GL072637.

Shanks, A.L., Shearman, R.K., 2009. Paradigm lost? Cross-shelf distributions of intertidal invertebrate larvae are unaffected by upwelling or downwelling. Mar. Ecol. Prog. Ser. 385, 189–204.

Strathmann, M.F., 1987. *Reproduction and development of marine invertebrates of the northern Pacific coast: Data and methods for the study of eggs, embryos, and larvae.* Seattle: University of Washington Press.

Thompson, B., Bergen, M., 1993. Population Biology of the Brittlestar. South. Calif. Coast. Water Res. Proj. Annu. Rep.

Underwood, A.J., Fairweather, P.G., 1989. Supply-side ecology and benthic marine assemblages. Trends Ecol. Evol. 4, 16–20.

Vargas, C.A., Escribano, R., Poulet, S., 2006. Phytoplankton food quality determines time windows for successful zooplankton reproductive pulses. Ecology 87 (12), 2992–2999.

Venables, W.N., Ripley, B.D., 2002. Modern Applied Statistics with S, fourth ed. Springer, New York.

Warn-Varnas, A., 2007. Water masses in the Monterey Bay during summer of 2000. Cont. Shelf Res. 27 (10–11), 1379–1398.

Wing, S.R., Botsford, L.W., Ralston, S.V., Largier, J.L., Woodbury, D., Sakuma, K., et al., 1998. Meroplanktonic distribution and circulation in a coastal retention zone of the northern California upwelling system. Limnol. Oceanogr. 43, 1710–1721.

Wilkerson, F.P., Dugdale, R.C., Kudela, R.M., Chavez, F.P., 2000. Biomass and productivity in Monterey Bay, California: contribution of the large phytoplankton. Deep Sea Res. Part II 47 (5–6), 1003–1022.

Wing, S.R., Botsford, L.W., Morgan, L.E., Diehl, J.M., Lundquist, C.J., 2003. Inter-annual variability in larval supply to populations of three invertebrate taxa in the northern California Current. Estuar. Coast. Shelf Sci. 57, 859–872.

Zeileis, Achim, Kleiber, C., Jackman, S., 2008. Regression Models for Count Data in R. J. Stat. Softw. 27 (8).